Rethinking Sampling-Based Fitness Measurement: Introducing Distributional Fitness Evaluation for Minimising Stochasticity and Anti-Symmetry

Zhenyue Qin, Tom Gedeon, R.I. (Bob) McKay

***Abstract*—EDIT REQUIRED: SEE SOURCE HERE Discrete gene regulatory network (GRN) plays a vital role in the study of robustness and modularity. A common method on evaluating the robustness of GRNs is to measure their capability of regulating a set of perturbed gene activation patterns back to their original forms. Traditional perturbations are obtained by collecting random samples produced by a predefined distribution of gene activation patterns. Such sampling method introduces stochasticity, which causes hardships in reproducibility, analytticity, and other post-experimental analyses. By contrast, in this paper, we develop a deterministic distributional fitness evaluation by considering the complete distribution of gene activity patterns to avoid stochasticity in fitness assessment. This novel fitness evaluation facilitates repeatability. Its determinism also endures the possibility of studying the theoretical maximum fitness. By utilising this new technique, we reveal an intrinsic symmetric structure within a widely-used model of studying evolvability, which we show experimentally can detriment its performance. We present a simple anti-symmetry mechanism and fully exhibit its efficacy including generating significantly more robust and modular networks, despite its simplicity. With our distributional fitness evaluation, we also unveil some properties of desirable GRNs in order to be robust and modular. We conclude this paper with a number of obscure phenomena remaining to be understood in the future.**

I. Introduction

EDIT REQUIRED: SEE SOURCE HERE

MOST applications of evolutionary optimisation rely on an abstracted mathematical model of the problem under consideration. The majority of real-world applications combine complex models (with correspondingly complex fitness functions) and noisy fitness evaluation. In most cases, this noise may be regarded as random sampling from a (more or less completely known) distribution. We may know some properties of this distribution even when we do not fully understand it or cannot directly evaluate it; in a subset of such problems, we may even be able to directly evaluate it. One important source of such problems is simulation of biological evolution. In this paper, we show how a distributional analysis of a specific evolutionary model can help to tease apart the effects of noise and of problem complexity, yielding a much better understanding of the behaviour of the evolutionary model. While doing so, we also discuss the generality of the techniques, and the extent to which they may be applicable to other problems in which properties of the noise distribution may be inferred.

A long-standing ambition of systems biology is to model and understand the mechanisms under which complex biological organisms operate [1]. That is, how can a large number of cells spontaneously organise and execute very complex behaviours [2], and why such biological systems exhibit a variety of desirable engineering features, such as fault tolerance, flexibility, despite being complex [3]. Understanding of these complex biological systems can not only address fundamental questions to our knowledge of essence of life, but will also lead to pragmatic innovations in medicine and engineering [4]. For example, deep artificial neural networks are derived from mathematically modelling the activities of human brains [5], and have shown great successes in a wide range of applications such as computer vision [6], game solving [7], and so on.

The study of systems biology consists of two-pronged approaches: knowledge discovery, also known as data mining, and simulation-based analysis [4]. The former extracts useful results from huge amounts of raw data in order to propose hypothesis to account for the generation of the data, which is an *in vitro* field [8]. By contrast, the latter builds mathematical models that share characteristics of natural biological processes, and verify the pre-proposed hypothesis *in silico* [9]. Hypotheses that were defended by *in vivo* simulations can further be tested with *in vitro* experiments for more definitive conclusions [10].

Although traditionally biological studies mainly focus on methods based on knowledge discoveries, simulation-based approaches have started raising an increasing attention [11]. This trend is due to three main reasons. First, mathematical biological models, compared to the descriptive ones used in discovery knowledge fields, are more rigorous and powerful [10]. Second, *in vivo* experiments can be challenging to conduct since characteristics of gene-gene interactions are hard to measure, change or control [12], [13]. Third, it can be infeasible to study dynamics and evolutions of organisms whose time scales are astonishing [14]. For instance, an analysis of the evolutionary stability can reach a macro-evolutionary time scale of a range from 10^7 to 10^8 generations [15]. In this paper, we discuss simulation-based in silico systems biology.

There are two distinct approaches of building formal math-

Z. Qin is with the Research School of Computer Science, Australian National University, Canberra, ACT 2600, Australia (e-mail: zhenyue.qin@anu.edu.au).

T. Gedeon is with the Research School of Computer Science, Australian National University, Canberra, ACT 2600, Australia (e-mail: tom@cs.anu.edu.au).

R.I. (Bob) McKay is with the Research School of Computer Science, Australian National University, Canberra, ACT 2600, Australia (e-mail: robert.mckay@anu.edu.au).

ematical models: ordinary differential equations (ODE) models [16], and discrete models [17]. In this paper, we study the latter due to its simplicity, intuitiveness, and increasing popularity [18]–[20]. Discrete models contain a wide range of types include (probabilistic) Boolean networks [21], [22], logical nets [23], Petri networks [24], cellular automata [25], and agent-based systems [26]. We study symmetry - a common property within these discrete models of investigating systems biology. We present mathematically rigorous definitions on what is symmetry and display how to leverage symmetry to analyse commonalities of instances of a model type and enhance the efficiency of evolutionary simulations.

One major mechanism that systems and evolutionary biologists aim to understand is robustness, which is a fundamental principle that underlines all levels of organisations within biological systems [27]. Robustness is a property that enables a system to maintain its functionalities despite facing internal and external perturbations [28]. In-depth understanding in robustness can shed light on the mechanism of how genetics and environment may combine to cause failures of homoeostasis, which can further guide interventions on how to restore them [29]. This understanding can also benefit artificial life and evolutionary computation, as engineers can leverage the mechanisms of robustness to solve traditionally intractable problems [30]. Taking networks as examples, biological systems and processes have evolved the capability of quickly adapting to the constantly varying environments as well as being robust to the failures caused by both internal and external errors [31].

A common method of studying robustness is to randomly sample a set of perturbed patterns and test whether the model can regulate the disturbed patterns back to their original forms [32]. This study method has been applied in a large quantity of discrete model types, such as Boolean networks [33], Hopfield networks [34], gene regulatory networks [35], and a lot more. Despite the fact that stochastic sampling is pragmatic, i.e., they mimic the non-deterministic process in nature, it can cause problems in theoretical analysis due to three reasons: Firstly, the stochasticity in sampling can cause difficulties in repeatability. Specifically, the same input can lead to different outputs under different experiments, trials, and even different timestamps within a trial; Secondly, the sampling non-determinism brings hardship in analysing optimality. That is, we hold uncertainty on whether a network displaying maximum fitness is due to noisy evaluation, or it is a true optimum; Thirdly, nature-like sampling can be computationally-consuming. For example, a human whose life expectation is 80 years can have more than $2 \cdot 10^{10}$ times of heart beats, which is intractable for a modern computer to conduct so many samples.

In this paper, we show the possibility of leveraging the entire distribution to analyse robustness of discrete system biological models in a maximally deterministic manner. We justify its feasibility from two perspectives:

1) Distributions from which the discrete model perturbations are sampled are analytically tractable, and can also be computational feasible for ordinal modern computers to traverse all the possibilities of the distribution. For example, the perturbation process of [35] essentially follows a binomial distribution, therefore the total possibilities is in the scale of $O(2^N)$, where N is the number of candidate perturbation locations, and is less than 15 in their experiments. Under such settings, modern computers are able to consider all the events within that distribution.
2) Even when N is too large and is beyond normal computational power to manage, we may still utilise the distribution by consider all the events that are highly probable, and conduct sampling for low-likelihood possibilities. This operation can significantly reduce the number of events to tackle, minimise the stochastic, and maximally employ information from the distribution.

We use Espinosa-Soto and Wagner (ES&W)'s discrete gene regulatory network model as an example, which is a variation of the original Wagner's gene regulatory network (GRN) model for studying evolvability[1] [15]. We choose this ES&W's GRN model due to the following three motivations: Firstly, Wagner's GRN model has witnessed great successes in a variety of computational biological studies [36]–[38]; Secondly, this model is specifically designed to study modularity, which is a mechanism which allows a system to contain damages locally for minimising the risks of system-wide malfunctions and considered to be a central question in systems biology [27], [39]; Thirdly, this model shares a large number of commonalities with Kauffman's discrete model [9], which is the origin of the following series of discrete models, yet Wagner's model is more powerful due to the consideration of transcriptional regulations [15]. Nonetheless, please note that the two proposed tools in this paper, namely anti-symmetry mechanism and distributional fitness analysis, applies to a much wider range of systems biological models. To be more specific, the anti-symmetry mechanism applies to a variety of discrete models and the distributional fitness evaluation is applicable to an assortment of perturbation-based robustness studies.

In summary, we outlines our contribution as following:

1) We show a new avenue of studying robustness by leveraging the entire perturbation distribution instead of the traditional sampling-based methods. Such approach can significantly reduce the experimental stochasticity and enhances reproducibility.
2) We formally define symmetry in discrete systems biological models and exhibit how to leverage symmetry to better understanding discrete biological model behaviours and improve efficiency of simulations.

The remainder of this paper is organised as follows. Section X ...

II. Related Work and Motivation

In this section, we present a brief overview of emergence of modularity, of GRNs and of Espinosa-Soto and Wagners [35] GRN Model. Then, we introduce the motivation of this paper. Finally, we give an explanation of symmetry in evolutionary

[1]Since we repeatedly need to refer to this crucial paper, we abbreviate it as ES&W

simulations and why it may be both biologically unrealistic, and detrimental to the simulated evolutionary process.

Judging by citations, the parsimony-based model of modularity emergence of Clune et al. [40] has of late been dominant. There is little doubt of its importance for evolving modular engineering systems, but its relevance to biology is more moot. Parsimony pressures have long been studied in genetic programming EDIT REQUIRED: SEE SOURCE HERE, yet are notoriously difficult to tune – too strong a pressure (relative to the primary objective) and one is left with tiny but highly unfit solutions; too weak, and complexity runs riot. Yet in biology, as Clune et al. argue, modularity is ubiquitous, yet there is no obvious mechanism to tune the many different parsimony pressures required to explain its widespread emergence. Clune et al. avoid this through use of the highly engineered NSGA-II multi-objective evolutionary algorithm EDIT REQUIRED: SEE SOURCE HERE, which is perfectly fine for engineering modularity in artificial systems, but questionable as a model of biological evolution (NSGA-II uses population-wide computations that would require a 'hidden hand' in biological systems). Thus at least in understanding biology, it is worth re-examining alternative explanations.

[35] traced the emergence of modularity to specialisation. It is based on Wagner's GRN model, which has witnessed wide application in a variety of computational biological studies [36]–[38]. It is important to acknowledge that their system also included a parsimony mechanism, but in the mutation operator, not as a second objective. This parsimony mechanism is not sufficient on its own to generate modularity, specialisation is required; equally important, the parsimony of the mutation operator requires little tuning, a wide range of values suffice.

A. Gene Regulatory Network (GRN)

A GRN is a collection of molecular regulators that coordinate interactions between genes (including both the protein-coding DNA sequences and regulatory non-coding DNA sequences), RNAs and proteins [41]. GRNs are central to the operation of all known forms of cellular life (eukaryota, bacteria and archaea [42]) and viruses [43]. The network structure of GRNs demonstrates a high level of modularity, considered to be a key contributor to robustness [44].

B. Espinsa-Soto and Wagner's GRN Model

The Espinosa-Soto and Wagner model [35] abstracts cellular homeostasis, in which a cell can recover from small perturbations to a target state and recover that state. It consists of two components, one or more targets, and the GRN itself. A target is a set of gene activation patterns, represented by a vector of N binary values, with $+1$ and -1 respectively representing activity and inactivity, so that there can be 2^N sates overall. Figure 1 depicts two target activation patterns consisting of 10 genes that happen to have a modular structure of two modules of five genes each; the activation in the first module of the patterns is identical (shared), but opposite in the second (divergent).

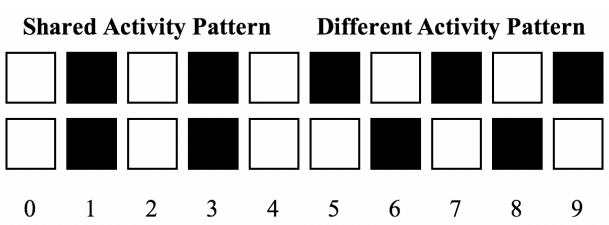

Fig. 1: A target consisting of two gene activation patterns, where white and black squares represent active $(+1)$ and inactive (-1) genes
EDIT REQUIRED: SEE SOURCE HERE

The gene state is regulated by a GRN g, which controls the activation pathway of the organism. For a pattern of N genes, it is abstracted as a ternary N^2 transition matrix $g = g_{ji}$ with entries over $\{-1, 0, 1\}$, representing repression, independence or activation of gene i by gene j. A gene activity pattern regulated by this network is a Boolean row vector $s = [s^0, ..., s^{N-1}]$. The state transition is modelled by:

$$A(g, s) = \sigma[g.s^{\mathrm{T}}] \tag{1}$$

where ${}^t extT$ represents matrix transposition and $\sigma(x) = 1$ if $x > 0$, $\sigma(x) = -1$ otherwise (applied elementwise).

Wagner's model focuses on the evolution of the $N \times N$ GRN matrix, generally by a typical evolutionary algorithm. This can lead to a terminological confusion. In the modeled biology, there are N genes in the activation pattern; but consdered at the evolutionary algorithm level, the evolving chromosome consists of N^2 genes. To alleviate confusion, we refer to the former as a "pattern gene", and the latter as a "network gene" or "network node". Figure 2 presents a flow chart of the fitness evaluation in the model.

In the rest of this paper, we will concentrate on the work of [35] with the target of figure 1, where an evolutionary system evolved first for 500 generations with a target consisting solely of the first activation pattern, and then for the remainder of the time (1500 further generations) with both activation patterns as target.

C. Anomalous Behaviours of the GRN Model and Our Motivation

Our initial work on this GRN model under typical genetic algorithm settings revealed a number of anomalies [45]. In summary, despite relatively fit, modular GRNs emerging in simulated evolutions, they could often be readily improved in both vitness and modularity by manually removing all inter-module connections, as in Figure 3. Yet evolutionary search does not find these improvements, despite mutation biases appearing to favour finding them. Figure 4 reveals that this is not due to discontinuous gradients: starting with the most robust/fittest GRN from the final generation of a typical run and removing non-modular edges one-by-one reveals a path of steadily improving fitness to a fully modular GRN. This phenomenon occurs even in runs incorporating elitism.

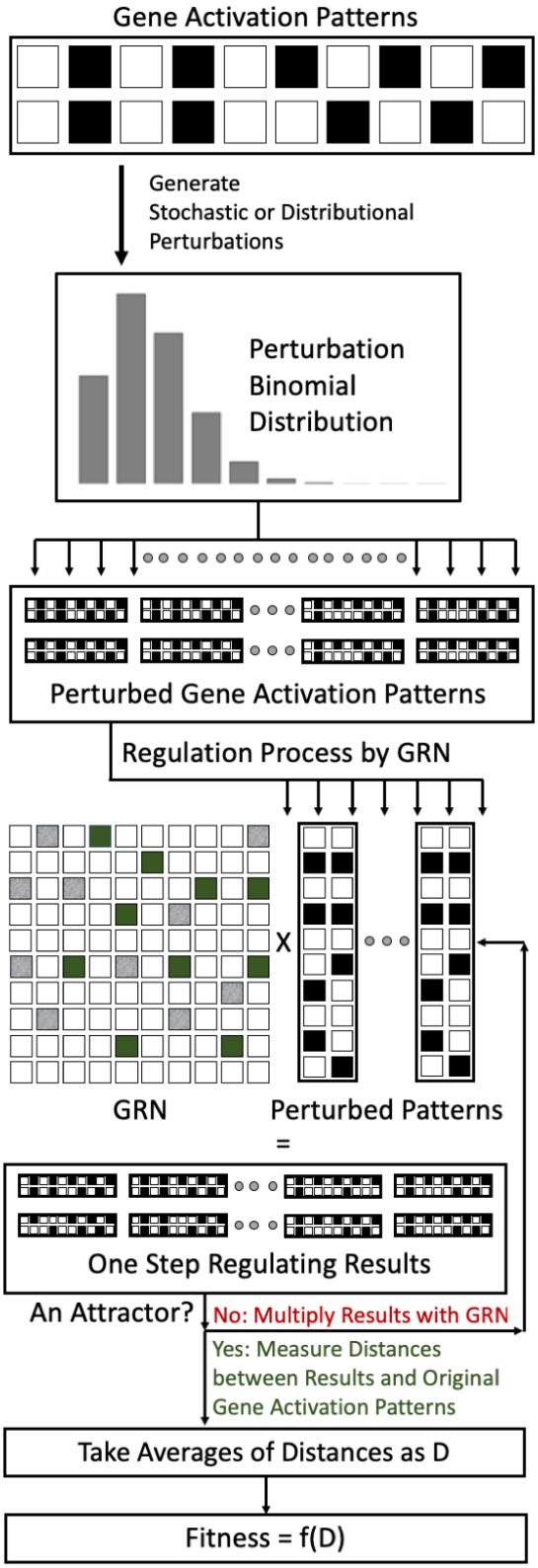

Fig. 2: Flow Chart of the Fitness Evaluation in [35]'s GRN model. Dark untextured squares represent activation, grey texture repression and white independence.

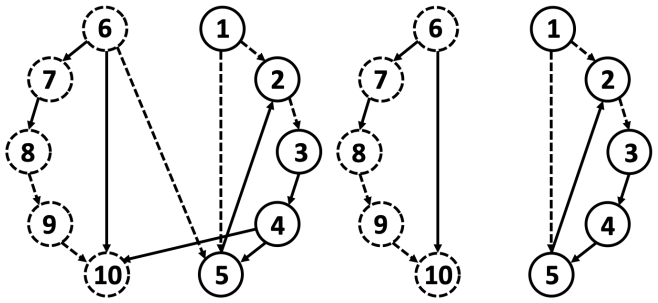

(a) Before Removal (b) After Removal

Fig. 3: Illustration of deterministically removing all the inter-module connections of a GRN. Solid and dashed circles represent different modules. Solid and dashed arrows stand for activation and repression respectively.

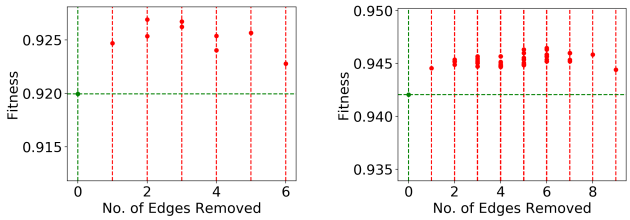

(a) With Elitism (b) Without Elitism

Fig. 4: Fitness increases continuously while removing inter-module connections from a fit GRN. Green dots represent the initial fitnesses, and red dots show the resulting fitnesses from inter-module connection removal.

D. Symmetry within Espinosa-Soto and Wagner's GRN Model

In evolutionary fitness landscapes, a symmetry is an invertible mapping that preserves distance and fitness.

The specific tagets used in [35] incorporates a number of symmetries. Within the activation patterns, locations $\{1, 3, 5\}$, $\{2, 4\}$, $\{6, 8, 10\}$ and $\{7, 9\}$ behave identically; this symmetry induces a symmetry on the GRN space. For example, the symmetry between locations 1 and 3 means that, in a GRN matrix, exchanging rows 1 and 3, and also columns 1 and 3, generates a symmetry on the search space. In fact, any permutation of these locations generates a symmetry, of which there are therefore $3 \times 2 \times 3 \times 2 = 36$.

Symmetry is well-known problem for evolutionary algorithms [46], partitioning the whole search space into multiple equivalence classes [47]. Figure 5 shows examples of symmetric and asymmetric landscapes; in the asymmetric case, despite its multiple local optima, individuals selection can concentrate the population on the higher peaks, whereas in the symmetric case concentration only occurs through random symmetry breaking.

It is easy to accidentally introduce symmetry into abstracted fitness landscapes. One of the take-home messages of this work is that this is generally disadvantageous, and symmetries should be deliberately avoided unless it is a characteristic of the real problem being abstracted.

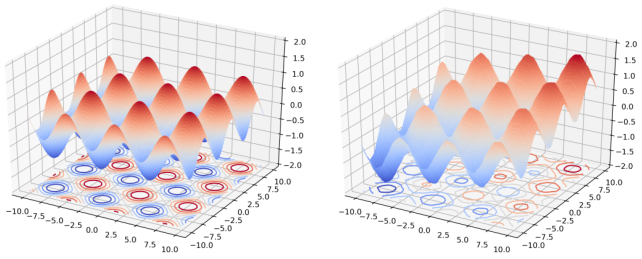

(a) Symmetric Landscape (b) Asymmetric Landscape

Fig. 5: Examples of symmetric and asymmetric landscapes.

Symmetry is a common outcome of evolution, so common that it is used to distinguish major biological groupings – among animals, between bilaterians, non-symmetric animals such as sponges, and rotationally symmetric animals; among flowering plants, according to the rotational symmetries of their flowers. But it is not so obvious that biological fitness landscapes exhibit symmetries. In the specific case of GRNs, there is no particular reason to suppose that one gene-gene interaction is of the same strength as another, or that variations in gene expressions have exactly the same quantitative effect at phenotypic level, it is at least not obvious that symmetries are as common as they are in artificial evolutionary systems. Thus it is worth studying the effects of these symmetries on a more micro level. We return to this later.

III. Distributional Fitness Evaluation

We hypothesised that the anomalies discussed in Section II-C might arise from the stochasticity of the sampling process of [35]: that in a population converged close to a local optimum, using order-based (tournament) selection, small stochastic variations in fitness might make it difficult to follow weak gradients. To evaluate this hypothesis, we need to separate the effects of the underlying fitness landscape from the effects of stochastic sampling. Fortunately, this is not hard to do, both in principle, and in this case, in practice.

In common with other GRN robustness models [48]–[50], [35] samples perturbations stochastically, then studies the recovery of the original pattern. [35] uses a binomial model: 500 perturbations of the locations in the pattern are identically and independently sampled, with a probability of being perturbed of $p = 0.15$, the recovery by each GRN genrates a reward based on the level of recovery, then the reward is averaged over the sampled perturbations. Thus we can compute the expected fitness of a GRN by tracing its behaviour over all 1024 possible perturbations, and weighting appropriately. This produces a deterministic fitness metric, and at a computational cost $1024/500$ (i.e. roughly double) that of [35]. We call this method distributional fitness evaluation. The underlying idea is extensible beryond discrete GRNs to a wide range of computational studies of discrete netwroks, including other genetic networks [51], Boolean neural networks [52], and Hopfield networks [53].

A. Definition and Advantages of Distributional Fitness Evaluation

Partially following the ideas of [35], we can extend the (one step) action $A(g, s)$ of an $N \times N$ GRN g on an activation state s of length N of equation 1 to its recursive application as

$$A^0(g, s) = s$$
$$A^{t+1}(g, s) = A(g, A^t(g, s))$$

We define an elementary perturbation e of length N as a vector of $\{-1, 1\}$, so that a perturbation of a target state s (also of length N) in the sense of [35] is the pairwise product $e \odot s$. Following Boolean usage, the weight $w(e)$ of an elementary perturbation is the number of -1 values.

[35] follows the regulatory process for $t_0 = 20$ steps:

$$G(g, e \odot s) = \begin{cases} s & \text{if } A^t(g, e \odot s) = s \text{ for } t < t_0 \\ A^{t_0}(g, e \odot s) & \text{otherwise} \end{cases} \tag{2}$$

and uses two auxiliary functions to weight contributions:

$$f(g) = 1 - e^{(-3 \cdot g)}$$
$$\gamma(x) = (1 - x)^5$$

Putting it together, we evaluate the effectiveness of GRN g in recovering state s as

$$F(g, s) = f\left(\sum_{n=0}^{N} p_n \cdot \frac{1}{|E_n|} \sum_{e \in E_n} \gamma\Big(H\big(G(g, e \odot s), s\big) \Big) \right) \tag{3}$$

where E_n is the set of elementary perturbations of length N and weight n, p_n is the probability $p_n \sim B(N, p)$ from the binomial distribution, and H is the Hamming distance.

EDIT REQUIRED: SEE SOURCE HERE

Compared with the random sampling of perturbations of [35], distributional fitness evaluation offers the following advantages:

1) Determinism: evaluating the fitness of a GRN multiple times will give the same fitness each time, while preserving essentially the same fitness landscape as sampling. This allows us to disentangle the effects of the fitness landscape itself, and that of noise.
2) Global Optimum Analysis: we can determine bounds on the fitness, and test whether those bounds are achieved; with a stochastically evaluated fitness, it is infeasible to determine whether further improvement is possible.
3) Speed Optimisation: Due to the determinism of fitness evaluation, cacheing of previously computed fitness may reduce wasted computation.

B. Upper Bounds on Distributional Fitness

An obvious upper bound for the fitness of a GRN in the scenario of [35] is for the GRN to return all perturbations of a target to the corresponding target. When there is only a single target, this is attainable (as we shall see), and for the 10×10 GRNs that are the focus of this study, is readily evolved. However we follow [35] in using a two-stage evolution, in the second stage of which there are two targets. In this case, this

upper bound is not attainable. It is easy to see why. Consider the first target of Figure 1. If it is perturbed by an elementary perturbation of weight 0 (i.e. it is unperturbed), then we would expect a GRN to readily recover it (it isn't required to do anything). But consider the second target perturbed by an elementary perturbation whose first five locations are 1, with the last five being -1. The resulting perturbed target is identical to the previous one. Hence the GRN must map it to the same end result: which is a Hamming distance of 5 from its target state. In fact, for every perturbation of target 1, there is a perturbation of target 2 that gives the same starting state for the GRN. At most one of them can be returned to its target by the GRN. Which choice is best?

To answer this question, consider the binomial probabilities of elementary perturbations by weight: to two decimal places: $< 0.20, 0.35, 0.28, 0.13, 0.04, 0.01, 0.00, 0.00, 0.00, 0.00, 0.00 >$. So perturbations of weights 0, 1 and 2 carry the most influence in equation 3, and for higher weights the influence decreases monotonically. Now for two elementary perturbations to conflict in this way, they must be identical in the first five places (since the two targets are identical there), and inverse on the last five (since the two targets are inverse there). So the choice is easy: the elementary perturbation with the least weight (therefore 0, 1 or 2) in the second half should be mapped back to the corresponding target. In this case, the Hamming distance between the regulated and original patterns is 0, and the result of function γ in Formula 3 is 1. Conversely, for second-half weights of 3, 4 or 5, the GRN will regulate the pattern to the opposite form. In such cases, the Hamming distance is 5 and γ returns 0.03125.

In summary, specialising equation 3 to the targets s_1 and s_2 of Figure 1 gives

$$\begin{aligned} &F(g) = \\ &f\Bigg(\sum_{n=0}^{10} B(n;10,0.15)\cdot \\ &\frac{1}{\binom{10}{n}} \sum_{e\in E_n : w_{6,10}(e)<3} \gamma\Big(H\big(G(g, e\odot s_1), s_1\big) \\ &+ H\big(G(g, e\odot s_2), s_2\big)\Big)\Bigg) \end{aligned} \tag{4}$$

where $w_{6,10}(e)$ denotes the weight of (number of -1's in) the second half of e.

Substituting values 1 and 0.03125 into Equation 4 and rearranging gives

$$\begin{aligned} &F(g) = f\Bigg(\sum_{n=0}^{10} B(n;10,0.15)\cdot \\ &\binom{10}{n}\cdot\Bigg(\sum_{e:w_{6,10}(e)<3} \cdot 1 + \sum_{e:w_{6,10}(e)>2} \cdot 0.03125\Bigg)\Bigg) \end{aligned} \tag{5}$$

Table I summarises how many elementary perturbations of each total weight have second half weights < 3 (resp. > 4). Substituting its values into Equation 5 gives a fitness bound to four decimal places of 0.9462.

TABLE I: Numbers of Unrecoverable Elementarty Perturbations by Weight.

Weight	No. of Perturbations	Unrecoverable
0	$\binom{10}{0}$	0
1	$\binom{10}{1}$	0
2	$\binom{10}{2}$	0
3	$\binom{10}{3}$	$\binom{5}{3}$
4	$\binom{10}{4}$	$\binom{5}{3}\cdot\binom{5}{1}+\binom{5}{4}$
5	$\binom{10}{5}$	$\binom{5}{3}\cdot\binom{5}{2}+\binom{5}{4}\cdot\binom{5}{1}+\binom{5}{5}$
6	$\binom{10}{6}$	$\binom{5}{3}\cdot\binom{5}{3}+\binom{5}{4}\cdot\binom{5}{2}+\binom{5}{5}\cdot\binom{5}{1}$
7	$\binom{10}{7}$	$\binom{5}{3}\cdot\binom{5}{4}+\binom{5}{4}\cdot\binom{5}{3}+\binom{5}{5}\cdot\binom{5}{2}$
8	$\binom{10}{8}$	$\binom{10}{8}$
9	$\binom{10}{9}$	$\binom{10}{9}$
10	$\binom{10}{10}$	$\binom{10}{10}$

C. Comparing Runs

EDIT REQUIRED: SEE SOURCE HERE

The treatments examined in this paper use a mixture of stochastic and distributional evaluation. How can we fairly compare them? In the long run, if the same individual is repeatedly re-evaluated using stochastic evaluation, the mean fitness must converge to the distributional fitness, in any particular case the stochastically evaluated fitness may be above or below the distributional fitness of the same individual. This would just induce noise in any comparisons (itself undesirable). However there is a further complication. We typically wish to compare the end-of-run best fitness achieved,, which introduces a bias: even if the same individual is produced as that best individual: since it was chosen as the best individual in the generation, in a stochastic evaluation run its fitness is more likely to have been stochastically evaluated in the upper part of the fitness distribution. To elminate this problem, for all comparisons, in all tables, and in all figures, except where explicitly mentioned, we always present the distributionally-evaluated fitness for an individual, even if it is evaluated using stochastic evaluation. This has the effect that for stochastic evaluation runs, figures showing the course of evoluation are not actually showing the fitness that was used in the evolution. The effect on a specific run can potentially be substantial. EDIT REQUIRED: SEE SOURCE HERE. However our results are typically averaged over 100 runs for a treatment. In this case, the stochastic variations may cancel out, and in our testing rarely exceeded ?? (a difference that would not be visibile in the figures presented).

D. Fitness Structure

EDIT REQUIRED: SEE SOURCE HERE

Figure 6 shows a typical ordered histogram over 100 runs of the mean best distributional fitness avhieved in the final generation (in this case, using distributional fitness evaluation as the objective). It is worth noting that the fitnesses are strongly suggestive of a plateau landscape (and in more detail,

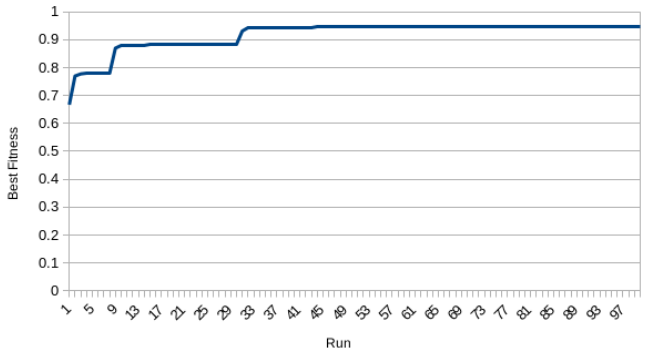

Fig. 6: Typical End-of-Run Best Fitness Distribution over 100 Runs

of multiple nested plateaux with further fine structure imposed on top. Essentially, this reflects the structure of the fitness evaluation: the primary plateau structure is determined by the success rate in restoring perturbations of size 1, there is a finer structure for perturbations of size 2, and so on for sizes 3 and 4. see teables for further detail (probably to supplementary material).

The consequence of this structure is that the primary metric we use in this paper, the mean over 100 runs of the best fitness in a generation, and in particular the final generation, is primarily determined by performance on the size 1 perturbations. This should be borne in mind in viewing the figures. We note also that if a run achieves optimum fitness on the 10 size 1 perturbations, it usually achieves optimal fitness on all perturbations. This strongly suggests that, at least close to global optima, the plateaux of different scales (i.e. corresponding to different-sized perturbations) are not in conflict: the problems are not deceptive in this case. However we see more fine structure when a run only succeeds with a smaller number of size 1 perturbations, suggesting that there may be more conflict between layers (i.e. greater deception) further from the global optima.

IV. Distributional ASymmetry GRN Model

In this section, we present a distributional ASymmetry (DAS-GRN) framework for an asymmetric version of Wagner's GRN model under distributional fitness evaluation, and briefly delineate the mutation and recombination operators.

A. Algorithmic Framework of DAS-GRN

Algorithm 1 presents a variant of the algorithm of [35], which is itself based on the classical haploid genetic algorithm [54]. It instantiates a Darwinism framework with discrete gene representation, selection, recombination, and mutation.

Algorithm 1: Algorithm Framework of DAS-GRN

Input: algorithm hyperparameters
population size Π of size
elitism rate H of rate (capital η)
mutation rate M of rate (capital μ)
generations Γ of number
per-location perturbation rate E of rate (capital ϵ)
asymmetric stepsize Z of size (capital ζ)
evolutionary tournament size T of size (capital τ)
Output: robust networks
`// Initialisation`
elite size $N_\epsilon = \Pi \cdot \mathrm{H}$;
crossover size $N_\chi = (\Pi - N_\epsilon)/2$;
generate Π feasible networks randomly;
save generated individuals in the population P;
get distributional fitness of each individual $I_i \in P$;
`// Loop until terminating condition`
for $i = 1$ *to* Γ **do**
  Reset $P' = \Phi$;
  select fittest N_ϵ individuals in P and save in P';
  `// Crossover`
  for $j = 1$ *to* N_χ **do**
    for $l = 1$ *to* 2 **do**
      for $k = 1$ *to* T **do**
        uniformly sample individual $I_{j,l,k} \sim P$;
      select $I_{j,l} = \mathrm{argmax}_{k \in \{1,\ldots,\mathrm{T}} F(I_{j,l,k})$;
    generate $I_{j,3}$ and $I_{j,4}$ from $I_{j,1}$ and $I_{j,2}$ by horizontal recombination;
    $P' = P' \bigcup \{I_{j,3}, I_{j,4}\}$;
  `// Mutation`
  foreach *individual* I_i *in* P' **do**
    if *mutation condition holds* **then**
      biasedly mutate I_i;
  `// Updating`
  get distributional fitness of each individual $I_i \in P'$;
  update $P = P'$;

B. Recombination

In [45], we introduced and experimentally investigated diagonal recombination. Given two parental GRNs $A_1[1, \ldots, 10]$ and $A_2[1, \ldots, 10]$, diagonal recombination proceeds by first sampling a pivot point i from $\{1, \ldots, 10\}$, then preserving the two sub-matrices $A_1[1 \ldots i-1, 1 \ldots i-1]$ and $A_1[i \ldots 10, i \ldots 10]$, while exchanging the remainder of corresponding locations between A_1 and A_2. This is illustrated in figure 7. We note that if i is sampled as 1, the corresponding recombination is a null operation.

C. Mutation

The mutation operator of [35] imposes a bias on the edge density to a specific, relatively low, level. A node in the network has a probability $\mu = 0.05$ to mutate every generation; if it mutates, it can either lose or gain an interaction. In matrix terms, the probability for each row to have a changed value is 0.05 (corresponding in the case of size 10 targets to a per-individual mutation rate, i.e. sampling a nonzero value from B(10,0.05), of approximately 0.4). The probability for a node to lose an interaction (a nonzero value to change to zero) is defined as

$$p(u) = \frac{4r_u}{4r_u + N - r_u} \tag{6}$$

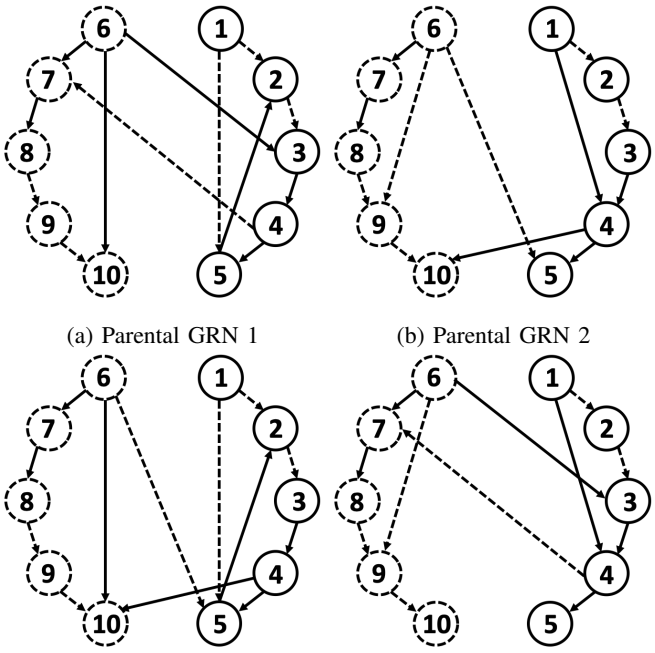

(a) Parental GRN 1 (b) Parental GRN 2

(c) Offspring GRN 1 (d) Offspring GRN 2

Fig. 7: Illustration of the diagonal recombination, with the pivot index as 5. Solid and dashed circles represent different modules. Solid and dashed arrows stand for activation and repression respectively.

where N is the number of genes in a gene activation pattern of a target, and r_u is the number of regulators of gene u [35], i.e. nonzero values in column u. Conversely, the probability for a gene u to gain an interaction (i.e. for a nonzero value in row u to become nonzero) is $1 - p(u)$. The neutral point of this bias can be computed as:

$$p(u) = 1 - p(u) \Rightarrow r_u = \frac{N}{5}$$

The bias acts to maintain the sparsity of the network at around this value, which research in computational biology suggests is essential to induce modularity [55].

V. Experimental Setup

All simulation code was implemented in Java 1.8.0 and Python 2.7.10. All programs are publicly available at EDIT REQUIRED: SEE SOURCE HERE We use the Mann-Whitney significance test in all comparisons. EDIT REQUIRED: SEE SOURCE HERE

A. Parameter Tables and Explanations

The specific targets T used in the experiments appear in Table II. Evolutionary and other simulation parameters for the main body of experiments are specified in Table III and explained in Table IV. A few variations on these will be specified in the relevant context.

TABLE II: Gene Activity Patterns (Target)

Target Pattern	Introduction Stage
+1 -1 +1 -1 +1 -1 +1 -1 +1 -1	0
+1 -1 +1 -1 +1 +1 -1 +1 -1 +1	500

TABLE III: Parameters of the Evolutionary Simulations

Pattern Size 10	GRN Size 100	Initial Density 0.2
# Perturbations 2^N or 500	Perturbation Rate 0.15	Population Size 100
Mutation Rate 0.05	Activation Rate 0.5	Crossover Rate 1.0
Crossover Type Diagonal	Selection (Size) Tournament (3)	Reproduction Rate 0
Elite Size 0 or 10	Max. Generation 2000	Asymmetry Gradient 0 or 0.01
Trials per Treatment 100	Significance Test Mann Whitney	

B. Population Initialisation

A population in our simulated evolution consists of 100 individuals, each being a GRN as defined in Eq 1. During initialisation, each individual in the population will randomly generate 20 edges with arbitrary directions for its GRN. The choice of number 20 comes from Eq. 6 that biases towards sparse networks as indicated in Subsection IV-C, Specifically, Eq. 6 shows each gene has 2 regulators and there are 10 genes, therefore the total edge number will be biased towards 20 in a GRN. Nonetheless, since the edge number lies in the range of 0 to 100 (the edges are directional), as to the probability mass function of edge number within a GRN, although the peak will locate at $p(e = 20)$, where p stands for probability

TABLE IV: Explanations of simulation parameters

Target Pattern	pattern to be perturbed then recovered
Introduction Stage	generations where target is introduced
Pattern Size	N, number of locations in an activation pattern
GRN Size	$N \times N$, the size of each GRN (evolved genotype)
Initial Density	initial density of edges in the GRN
# Perturbations	number of perturbations of each target[a]
Perturbation Rate	expected proportion of corrupted genes
Population Size	the number of individuals in the population
Mutation Rate	probability GRN node gains/loses an interaction[b]
Activation Rate	proportion of new interactions that are activations[c]
Crossover Rate	proportion of individuals that are crossed over[d]
Crossover Type	the tupe of crossover (recombination) used
Selection (size)	the type of selection and size when relevant
Reproduction Rate	proportion of old generation randomly copied on
Elite size	number of fittest individuals automatically copied
Max. generation	the generation when the simulation will terminate
Asymmetry Gradient	the gradient δ for symmetry breaking[e]
Trials per Treatment	number of trials for comparing treatments
Significance Test	statistical test used in comparing treatments

a For distributional evaluation, this will be 2^N.
b For compatibility with the terminology of [35]. In EC terms: the per-gene mutation rate in the evolving GRN is $1/N$ of this the per-individual mutation rate is N times this
c Gained interactions are either activations or repressions.
d Some crossovers may be ineffective, see subsection IV-B.
e From Equation **??**

and e represents edge number, the function curve will skew to the right part. Formally,

$$\sum_{e=0}^{20} p(e) < \sum_{e=21}^{100} p(e)$$

As a result, the expected number of edges within a GRN may not be exactly 20, which despite being biased towards. We conducted empirically experiments by not applying selection pressure to the simulated evolutions, which exhibit the expected GRN edge number is approximately 22.

C. Selection Scheme: Tournament vs Proportional Selections

There are two prevailing selection schemes: tournament and proportional selections. Despite the fact that ES&W employee proportional one [35], we utilise tournament in this paper and provide rationale behind this choice. We turn recombination off in the experiments of comparing tournament and proportional in order to minimise influences from other evolutionary operators except selection schemes. The results are in Figure 8. As to the best fitness in each generation, tournament selection can preserve them better than proportional one, *i.e.*, , the highest fitness in the next generation is less likely to decrease. Furthermore, compared with proportional selection, the median fitness of tournament in each generation is higher with a large margin for tournament one.

D. Modularity Metric

We adopt the modularity Q scoring system to quantify modularity in a GRN, based on the algorithm proposed by Newman [56]. Briefly, this approach is defined as the difference between the ratio of the number of edges in the network connecting nodes within a module over the number of all the edges, and the same quantity when assigning the nodes into the same modules yet edges are assumed to be randomly connected in the network [57]. Formally, Q is calculated as

$$Q = \sum_{i}^{K} [\frac{l_i}{L} - (\frac{d_i}{2L})^2] \tag{7}$$

where i represents one of the K potential modules within a network, L is the total number of connections in a network, l_i stands for the number of interactions in the module i, and d_i is the sum of degrees of all the nodes in module i [35]. The value Q will sit in the range of $[-0.5, 0.5]$ for our particular case.

Nonetheless, the typical definition of modularity Q varies according to the total number of edges. In order to alleviate the variations from total edge numbers within a GRN, we normalise Q as Eq. 8, following the spirit of [57] for a fair comparison.

$$Q_n = \frac{Q - Q_{ran}}{Q_{max} - Q_{ran}} \tag{8}$$

where Q is the modularity Q value obtained from Eq. 7 for a certain network $\{V, E\}$, Q_{ran} is the average Q value of 10,000 random networks with the same number of nodes V and edges E as the network $\{V, E\}$, and Q_{max} stands for the maximum Q value in these 10,000 random networks. This normalised Q_n shows us how modular our network is by comparing to the random networks with the same attributes [35].

VI. Experimental Results and Analysis: Stochastic vs Deterministic Evaluation

In the first set of experiments, we compare the behaviour of the algorithm using stochastic evaluation with that using distributional evaluation. From the perspective of the particular domain, it helps to understand to what extent aspects of the behaviour (for example, emergence or non-emergence of modularity) are a consequence of the fitness landscape of the problem, and to what extent they derive from the noise effects of random sampling imposed upon that landscape. From an evolutionary biology perspective, they allow us to compare the behaviour of small population and perturbation sample sizes that are computationally tractable but generally biologically implausible against the smoothing effect of effectively infinite perturbation samples. Because a key effect of incresing either population size or perturbation sample size is to smooth behaviour, this can help to gain some insight into what we might expect from more biologically realistic (but computationally infeasible) population sizes. Finally, from a methodolical perspective, this section illustrates what is feasible if the distribution underlying the noise is small enough to be directly computable (in this case, the GRN target is sufficiently short). Without further theoretical advances, the experiments would not be computationally tractable if the target, and thus the distribution, was much larger.

We conducted 100 independent evolutionary simulations for distributional and for stochastic fitness evaluation. We collected the fittest GRNs in each generation and evaluated their fitnesses and modularities. We remind readers that these results are reported using the distributional fitness, even for runs using stochastic evaluation. An important consequence is that we know, for stochastic runs, whether we have actually found an optimum.

A. Effects of Stochastic Evaluation on Evolutionary Efficiency

TABLE V: Mean Best Fitnesses and Modularity Q Values of Fittest GRNs (over 100 runs) from the Final Generation, for Distributional vs Stochastic Fitness Evaluation

	Distributional	Stochastic	p-value
Fitness	0.9171	0.9233	0.0636
Distributional Equivalent		0.9232	
Modularity	0.8516	1.0987	0.0074

1) Results: Table V shows the outcomes for fitness and modularity, while the top panels of figures 9 and 10 show the evolution of fitness and modularity over the generations.

Stochastic fitness evaluation has a positive effect on the fitness of the final generation best individual, though the difference does not reach statistical significance. For completeness, in the table we also show the fitness that the stochastic best individuals recorded using stochastic evaluation (in fact the difference is almost imperceptible). Stochastic

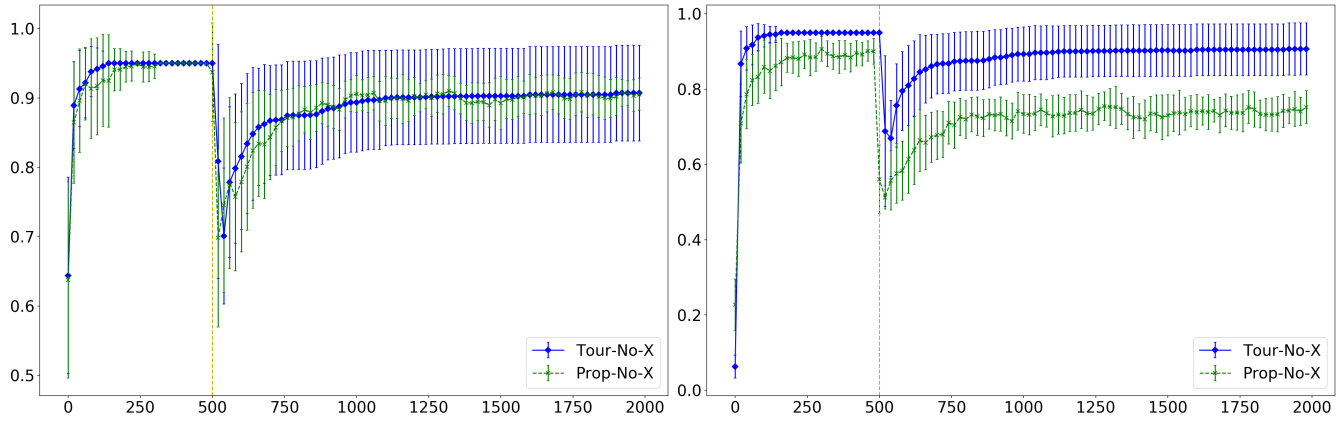

(a) Best Fitness in Every Generation.

(b) Median Fitness in Every Generation.

Fig. 8: Best and median fitness in every generation of evolutions without recombination for comparing the performance of tournament and proportional selections. Blue dots stand for tournament and green crosses represent tournament.

evaluation achieves a (distributional) fitness only 0.0229 below the theoretical bound of 0.9462, while distributional fitness evaluation is 0.0391 below. However the difference in modularity Q values is statistically significant, so stochastic noise in evaluation clearly benefits modularity, probably by generating broader search on the vast plateaux of fitness. In the graphs of fitness evolution, figures 9 and 10 suggest that fitness and modularity evolve similarly up to the change to the more complex target at generation 500; immediately after that, the noise from stochastic evaluation results in slower improvement, and less between-run variance, in both fitness and modularity, but improvement continues for longer, resulting in higher values by termination at generation 2000.

2) Analysis: It seems plausible here that greater stochasticity reduces eagerness in search and encourages exploration, resulting in higher fitness, and as a by-product, greater modularity. To test this, we decided to reduce eploration further by incorporating elitism.

B. Elitism may Damage Modularity

TABLE VI: Fitnesses of Fittest GRNs from the Final Generation with and without Elitism

Fitness	Distributional	Stochastic	Distributional Equivalent
Non-elite	0.9171	0.9233	0.9232
Elite	0.8912	0.9326	0.9327
p-value	$2.6518 \cdot 10^{-5}$	0.8364	
Modularity	**Distributional**	**Stochastic**	
Non-elite	0.8132	0.9454	
Elite	0.4480	0.8816	
p-value	$2.4567 \cdot 10^{-10}$	0.0253	

1) Results: Table VI and the top panels of Figures 11 and 12 show the comparative results between elitist and non-elitist strategues for both distributional and stochastic evaluation. Elitism substantially, and significantly, lowers fitness within the distributional algorithm, and as a result, also substantially and significantly reduces modularity. This strongly supports the hypothesis that wide exploration is desirable for this problem, and that getting stuck in local optima is worsened by elitism. Conversely, for stochastic evaluation, elitism showed a non-significant improvement in both fitness and modularity.

2) Analysis: Why should elitism make such a difference to the distributional results in the presence of distributional (i.e. fixed) evaluation, but not in the context of stochastic evaluation? It is worth noting that in a stochastic context, elitism does not truly function as intended. Under stochastic evaluation, the determination of the elite individuals is iteelf stochastic, and biasedly so (the individuals determined to be the elite are likely to have been evaluated, by chance, at the top of their stochastic range), so that there may be little loss in exploratory capacity by comparison with a context where each individual has a fixed (distributional) fitness.

C. Deterministic Fitness Evaluation with Complete Sampling Can Help Better Analysing GRN Edge Functions

In previous work [58] and [45], we reported that the simple procedure of manually removing inter-module edges from evolved highly fit but non-modular solutions could, in the majority of cases (24/40), further improve their fitnesses. We were puzzled by this phenomenon, because we expected that this procedure – favoured by the mutation bias – should be easily followed by an evolutionary algorithm. Using the deterministic distributional fitness evaluation, we determined that this scenario was mainly due to the stochasticity of the original fitness evaluation. Over 100 runs with distributional fitness evaluation, we collected the 100 fittest GRNs from the final generation. Among these, we manually removed any inter-module edges and measured the resulting fitnesses. Under distributional evaluation, only 7/100 had an improved fitness. However under stochastic evaluation, the imposed noise meant that 36/100 GRNs appeared to improve their fitness by undergoing this procedure. Thus in most cases, the

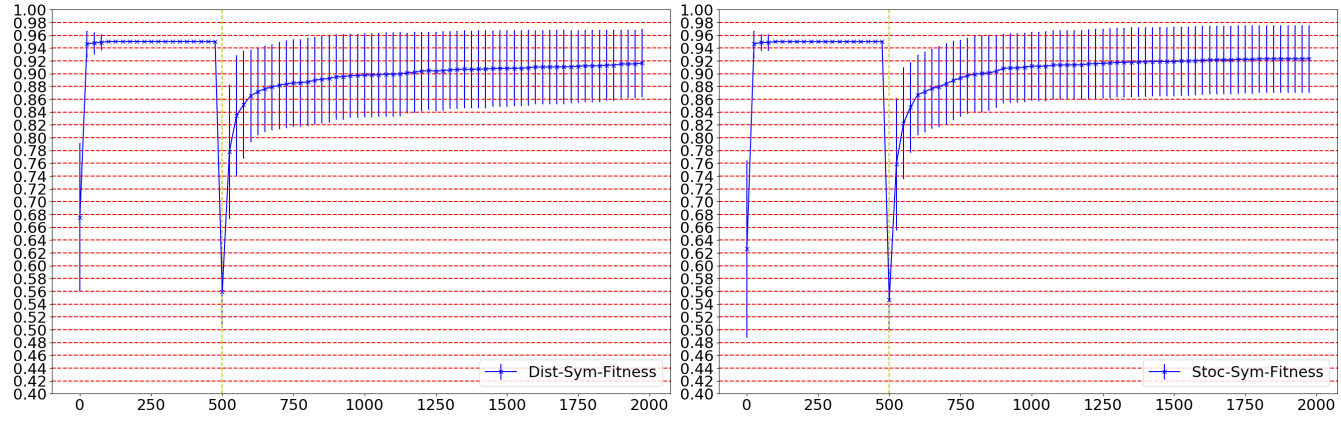

(a) Symmetric Distributional Fitness

(b) Symmetric Stochastic Fitness

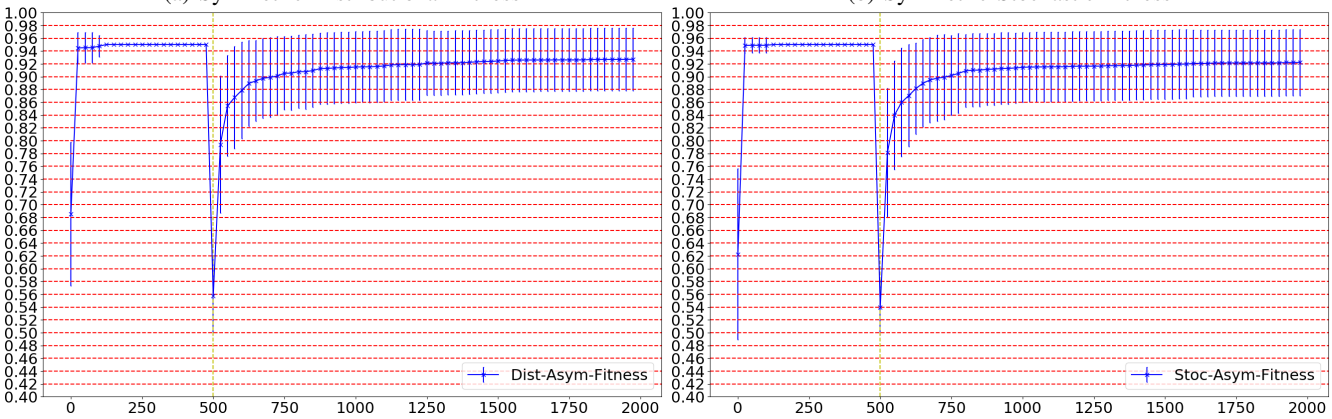

(c) Asymmetric Distributional Fitness

(d) Asymmetric Stochastic Fitness

Fig. 9: Mean Best Fitness for each Generation over 100 Trials. Left to Right: Distributional vs Stochastic Evaluation. Top to Botom: Symmetric vs Asymmetric Fitness Function. Vertical bars represent one standard deviation. The vertical dashed line at generation 500 denotes addition of the second activation pattern.

improvement was purely illusory; the few cases where there was a real (i.e. distributional) improvement in fitness were more than counterbalanced by the large number of cases where there was a deterioration.

VII. Characteristics of the GRN Model

EDIT REQUIRED: SEE SOURCE HERE In this section, we present our understanding of characteristics of ES&W's GRN model. We also exhibit some behaviours of this GRN model that we cannot comprehend even assisted with our distributional fitness evaluation. We leave them here as future work.

A. The GRN Regulating Process Are Based on A Majority Voting Problem

We noticed that during a single step of GRN regulation, each gene in the activation pattern independently. Along regulating, $+1$ and -1 node in a GRN intends to maintain and opposite the original gene value in the activation, respectively, which can be regarded as a majority voting process. Therefore, the GRN like Eq. 9 can act as an ideal solution for regulating a target containing two activation patterns [+1, -1, +1, -1, +1] and [-1, +1, -1, +1, -1]. Furthermore, we hypothesize that a necessary condition of an ideal GRN for this problem domain of regulating perturbed activation patterns can be that it has to be capable of solving the majority voting problem.

$$\begin{bmatrix} +1 & -1 & +1 & -1 & +1 \\ -1 & +1 & -1 & +1 & -1 \\ +1 & -1 & +1 & -1 & +1 \\ -1 & +1 & -1 & +1 & -1 \\ +1 & -1 & +1 & -1 & +1 \end{bmatrix} \tag{9}$$

B. Simulations Starting with Globally Optimal GRNs with Perfect Modularity Can Maintain Globally Optimal GRNs

Instead of randomly generating initial GRNs at the starting point of the evolution, we manually initialize the starting a population of GRNs that have two characteristics:

1) Its fitness is globally optimal.
2) Its modularity is perfect, i.e., there is no edge between modules.

We abandoned Phase I of the evolution and only kept Phase II during which GRNs had to simultaneously regulate two activation patterns containing both sharing and divergent genes. As a consequence, as Figure 13 and 14 indicated, the evolution could preserve the optimal fitness in each further generation, and maintain modularity in a relatively high level.

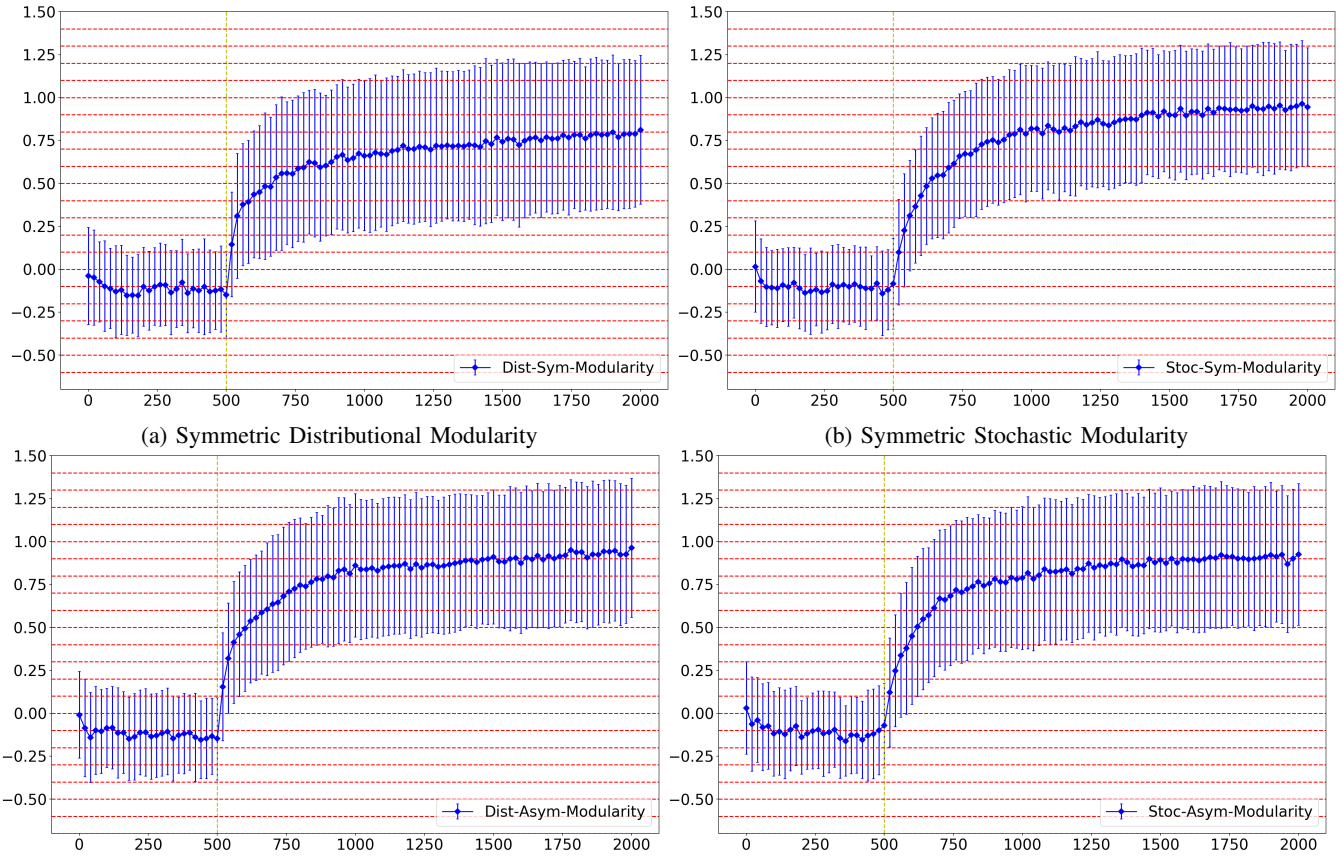

(a) Symmetric Distributional Modularity

(b) Symmetric Stochastic Modularity

(c) Asymmetric Distributional Modularity

(d) Asymmetric Stochastic Modularity

Fig. 10: Mean Modularity for each Generation over 100 Trials. Left to Right: Distributional vs Stochastic Evaluation. Top to Botom: Symmetric vs Asymmetric Fitness Function.

Furthermore, GRNs generated with the evolution with the perfect fitness and modularity initialisation contained much fewer edges than the previous evolution containing two stages, as Figure 15 showed, where the average edge number for the fittest GRNs in the final generation of 100 independent simulations were 23.3545 and 17.8046 for the previous and perfect-starting evolutions respectively (Mann Whitney Test: $p = 1.3123 \times 10^{-17}$). Further investigations are required to understand this phenomenon.

REFERENCES

[1] I. Tavassoly, J. Goldfarb, and R. Iyengar, "Systems biology primer: the basic methods and approaches," *Essays in biochemistry*, vol. 62, no. 4, pp. 487–500, 2018.

[2] K. Saetzler, C. Sonnenschein, and A. M. Soto, "Systems biology beyond networks: generating order from disorder through self-organization," in *Seminars in cancer biology*, vol. 21, no. 3. Elsevier, 2011, pp. 165–174.

[3] C.-M. Pintea, "Bio-inspired computing," in *Advances in Bio-inspired Computing for Combinatorial Optimization Problems*. Springer, 2014, pp. 3–19.

[4] H. Kitano, "Computational systems biology," *Nature*, vol. 420, no. 6912, p. 206, 2002.

[5] I. Goodfellow, Y. Bengio, and A. Courville, *Deep learning*. MIT press, 2016.

[6] A. Krizhevsky, I. Sutskever, and G. E. Hinton, "Imagenet classification with deep convolutional neural networks," in *Advances in neural information processing systems*, 2012, pp. 1097–1105.

[7] D. Silver, J. Schrittwieser, K. Simonyan, I. Antonoglou, A. Huang, A. Guez, T. Hubert, L. Baker, M. Lai, A. Bolton *et al.*, "Mastering the game of go without human knowledge," *Nature*, vol. 550, no. 7676, p. 354, 2017.

[8] P. Baldi, S. Brunak, and F. Bach, *Bioinformatics: the machine learning approach*. MIT press, 2001.

[9] S. A. Kauffman, "Metabolic stability and epigenesis in randomly constructed genetic nets," *Journal of theoretical biology*, vol. 22, no. 3, pp. 437–467, 1969.

[10] B. Di Ventura, C. Lemerle, K. Michalodimitrakis, and L. Serrano, "From in vivo to in silico biology and back," *Nature*, vol. 443, no. 7111, p. 527, 2006.

[11] R. A. Hillmer, "Systems biology for biologists," *PLOS Pathogens*, vol. 11, no. 5, pp. 1–6, 05 2015. [Online]. Available: https://doi.org/10.1371/journal.ppat.1004786

[12] T. Hindré, C. Knibbe, G. Beslon, and D. Schneider, "New insights into bacterial adaptation through in vivo and in silico experimental evolution," *Nature Reviews Microbiology*, vol. 10, no. 5, p. 352, 2012.

[13] Z. Paroo and D. R. Corey, "Challenges for rnai in vivo," *TRENDS in Biotechnology*, vol. 22, no. 8, pp. 390–394, 2004.

[14] D. E. Dykhuizen, "Experimental studies of natural selection in bacteria," *Annual Review of Ecology and Systematics*, vol. 21, no. 1, pp. 373–398, 1990.

[15] A. Wagner, "Does evolutionary plasticity evolve?" *Evolution*, vol. 50, no. 3, pp. 1008–1023, 1996.

[16] T. Q. Chen, Y. Rubanova, J. Bettencourt, and D. K. Duvenaud, "Neural ordinary differential equations," in *Advances in Neural Information Processing Systems*, 2018, pp. 6571–6583.

[17] S. A. Kauffman, *The origins of order: Self-organization and selection in evolution*. OUP USA, 1993.

[18] Ö. Sahin, H. Fröhlich, C. Löbke, U. Korf, S. Burmester, M. Majety, J. Mattern, I. Schupp, C. Chaouiya, D. Thieffry *et al.*, "Modeling erbb receptor-regulated g1/s transition to find novel targets for de novo trastuzumab resistance," *BMC systems biology*, vol. 3, no. 1, p. 1, 2009.

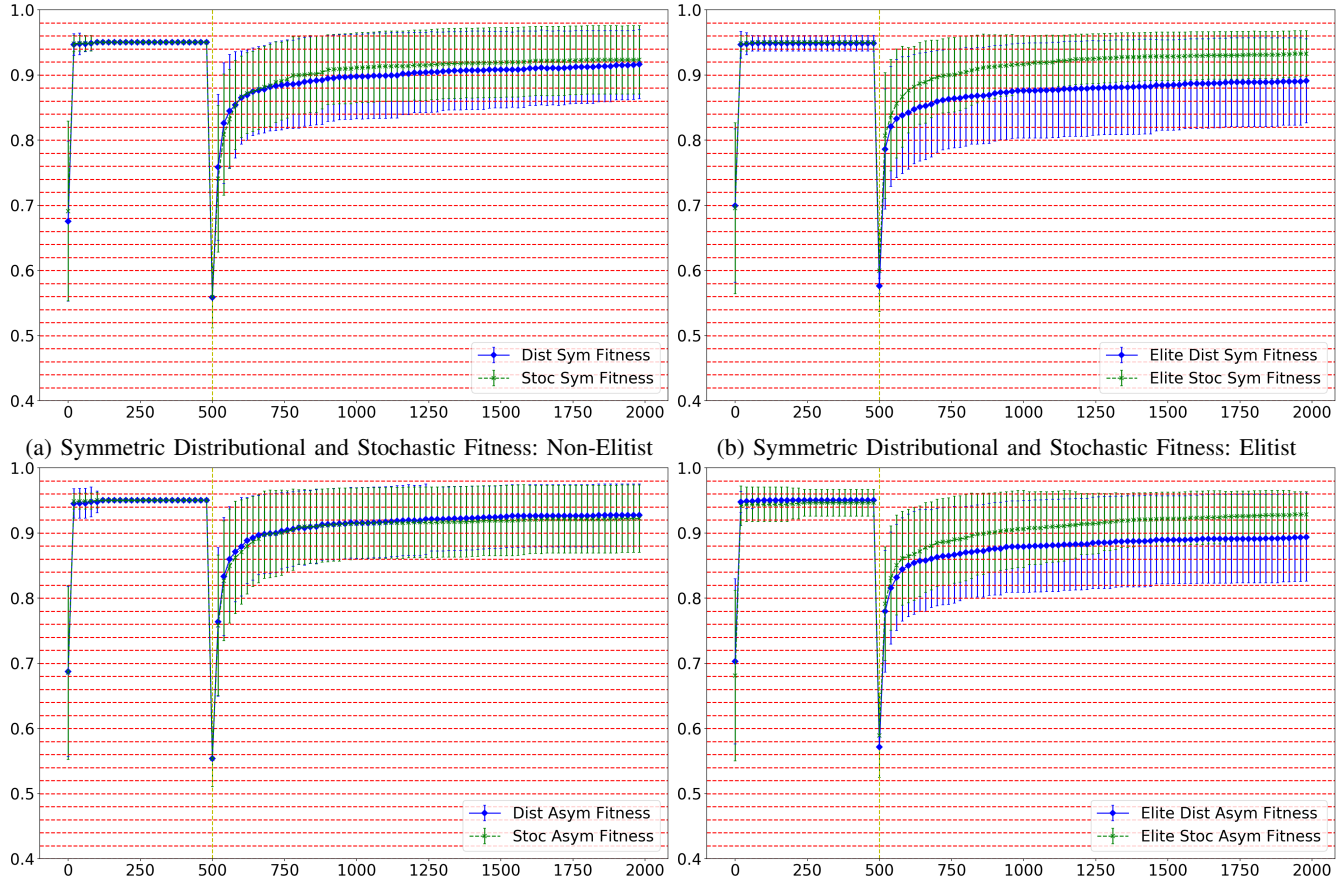

(a) Symmetric Distributional and Stochastic Fitness: Non-Elitist

(b) Symmetric Distributional and Stochastic Fitness: Elitist

(c) Asymmetric Distributional and Stochastic Fitness: Non-Elitist

(d) Asymmetric Distributional and Stochastic Fitness: Elitist

Fig. 11: Mean Best Fitness for each Generation over 100 Trials. Left to Right: Non-Elitist vs Elitist Algorithm. Top to Botom: Symmetric vs Asymmetric Fitness Function.

[19] L. M. Heiser, N. J. Wang, C. L. Talcott, K. R. Laderoute, M. Knapp, Y. Guan, Z. Hu, S. Ziyad, B. L. Weber, S. Laquerre *et al.*, "Integrated analysis of breast cancer cell lines reveals unique signaling pathways," *Genome biology*, vol. 10, no. 3, p. R31, 2009.

[20] L. Calzone, L. Tournier, S. Fourquet, D. Thieffry, B. Zhivotovsky, E. Barillot, and A. Zinovyev, "Mathematical modelling of cell-fate decision in response to death receptor engagement," *PLoS computational biology*, vol. 6, no. 3, p. e1000702, 2010.

[21] R. Albert and H. G. Othmer, "The topology of the regulatory interactions predicts the expression pattern of the segment polarity genes in drosophila melanogaster," *Journal of theoretical biology*, vol. 223, no. 1, pp. 1–18, 2003.

[22] I. Shmulevich, E. R. Dougherty, S. Kim, and W. Zhang, "Probabilistic boolean networks: a rule-based uncertainty model for gene regulatory networks," *Bioinformatics*, vol. 18, no. 2, pp. 261–274, 2002.

[23] A. W. Burks and J. B. Wright, "Theory of logical nets," *Proceedings of the IRE*, vol. 41, no. 10, pp. 1357–1365, 1953.

[24] V. N. Reddy, M. L. Mavrovouniotis, M. N. Liebman *et al.*, "Petri net representations in metabolic pathways." in *ISMB*, vol. 93, 1993, pp. 328–336.

[25] S. Wolfram, "Statistical mechanics of cellular automata," *Reviews of modern physics*, vol. 55, no. 3, p. 601, 1983.

[26] R. Laubenbacher, A. Jarrah, H. Mortveit, and S. Ravi, "Encyclopedia of complexity and system science," 2009.

[27] H. Kitano, "Systems biology: a brief overview," *science*, vol. 295, no. 5560, pp. 1662–1664, 2002.

[28] ——, "Biological robustness," *Nature Reviews Genetics*, vol. 5, no. 11, p. 826, 2004.

[29] J. Stelling, U. Sauer, Z. Szallasi, F. J. Doyle III, and J. Doyle, "Robustness of cellular functions," *Cell*, vol. 118, no. 6, pp. 675–685, 2004.

[30] F. Dressler and O. B. Akan, "Bio-inspired networking: from theory to practice," *IEEE Communications Magazine*, vol. 48, no. 11, 2010.

[31] S. Binitha, S. S. Sathya *et al.*, "A survey of bio inspired optimization algorithms," *International Journal of Soft Computing and Engineering*, vol. 2, no. 2, pp. 137–151, 2012.

[32] K. Wang and A. N. Michel, "Robustness and perturbation analysis of a class of artificial neural networks," *Neural networks*, vol. 7, no. 2, pp. 251–259, 1994.

[33] J. Aracena, E. Goles, A. Moreira, and L. Salinas, "On the robustness of update schedules in boolean networks," *Biosystems*, vol. 97, no. 1, pp. 1–8, 2009.

[34] J. J. Hopfield, "Neurons with graded response have collective computational properties like those of two-state neurons," *Proceedings of the national academy of sciences*, vol. 81, no. 10, pp. 3088–3092, 1984.

[35] C. Espinosa-Soto and A. Wagner, "Specialization can drive the evolution of modularity," *PLoS computational biology*, vol. 6, no. 3, p. e1000719, 2010.

[36] A. Bergman and M. L. Siegal, "Evolutionary capacitance as a general feature of complex gene networks," *Nature*, vol. 424, no. 6948, p. 549, 2003.

[37] R. B. Azevedo, R. Lohaus, S. Srinivasan, K. K. Dang, and C. L. Burch, "Sexual reproduction selects for robustness and negative epistasis in artificial gene networks," *Nature*, vol. 440, no. 7080, p. 87, 2006.

[38] E. Huerta-Sanchez and R. Durrett, "Wagner's canalization model," *Theoretical population biology*, vol. 71, no. 2, pp. 121–130, 2007.

[39] G. P. Wagner, M. Pavlicev, and J. M. Cheverud, "The road to modularity," *Nature Reviews Genetics*, vol. 8, no. 12, p. 921, 2007.

[40] J. Clune, J.-B. Mouret, and H. Lipson, "The evolutionary origins of modularity," *Proc. R. Soc. B*, vol. 280, no. 1755, p. 20122863, 2013.

[41] Y. Xiao, "A tutorial on analysis and simulation of boolean gene regulatory network models," *Current genomics*, vol. 10, no. 7, pp. 511–525, 2009.

[42] K. Nowick and L. Stubbs, "Lineage-specific transcription factors and the evolution of gene regulatory networks," *Briefings in Functional*

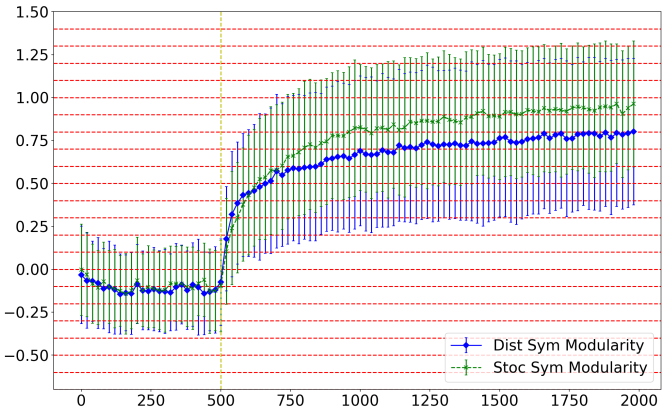

(a) Symmetric Distributional and Stochastic Modularity: Non-Elitist

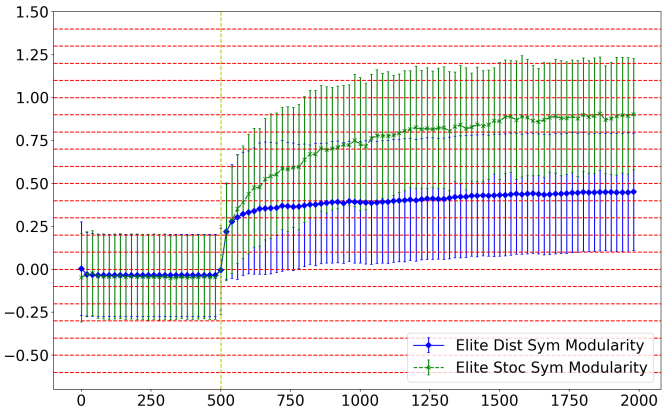

(b) Symmetric Distributional and Stochastic Modularity: Elitist

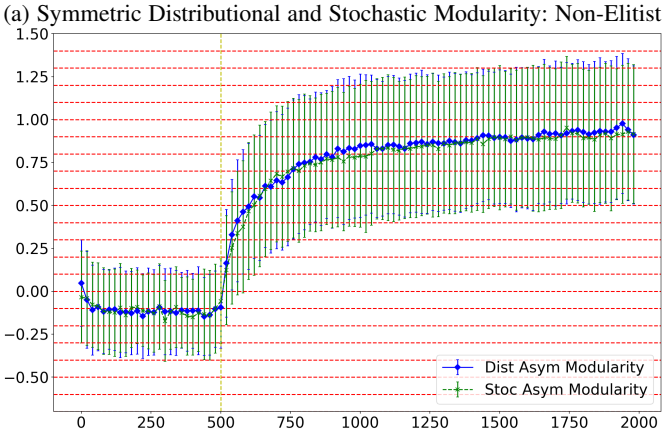

(c) Asymmetric Distrib. and Stochastic Modularity: Non-Elitist

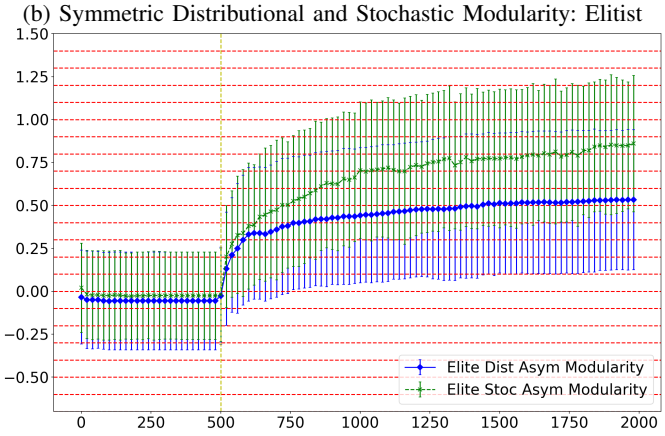

(d) Asymmetric Distributional and Stochastic Modularity: Elitist

Fig. 12: Mean Modularity for each Generation over 100 Trials. Left to Right: Non-Elitist vs Elitist Algorithm. Top to Botom: Symmetric vs Asymmetric Fitness Function.

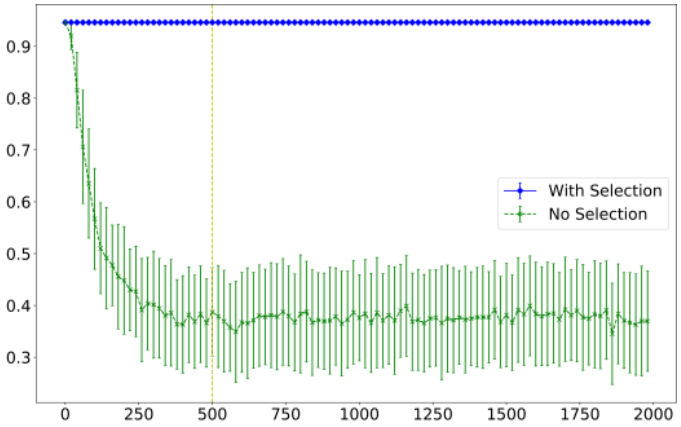

Fig. 13: Starting from the fitness and modularity optimal GRNs, the evolution could maintain the global fitness.

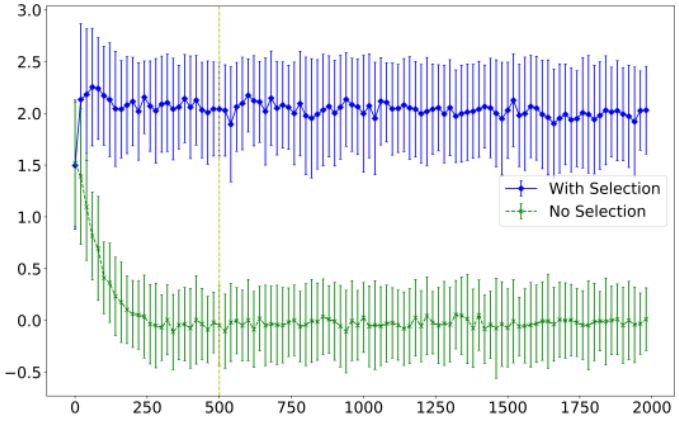

Fig. 14: Starting from the fitness and modularity optimal GRNs, the evolution could maintain a relatively higher modularity.

Genomics, vol. 9, no. 1, pp. 65–78, 01 2010. [Online]. Available: https://doi.org/10.1093/bfgp/elp056

[43] A. Bensussen, C. Torres-Sosa, R. A. Gonzalez, and J. Díaz, "Dynamics of the gene regulatory network of hiv-1 and the role of viral non-coding rnas on latency reversion," *Frontiers in physiology*, vol. 9, pp. 1364–1364, Sep 2018, 30323768[pmid]. [Online]. Available: https://pubmed.ncbi.nlm.nih.gov/30323768

[44] H. Kirsten and P. Hogeweg, "Evolution of networks for body plan patterning; interplay of modularity, robustness and evolvability," *PLoS computational biology*, vol. 7, no. 10, p. e1002208, 2011.

[45] Z. Qin, T. Gedeon, and R. B. McKay, "Anomalies in the behaviour of a modularity inducing problem domain," in *Artificial Life Conference Proceedings*. MIT Press, 2019, pp. 214–221.

[46] R. Santana, R. I. McKay, and J. A. Lozano, "Symmetry in evolutionary and estimation of distribution algorithms," in *2013 IEEE Congress on Evolutionary Computation (CEC)*. IEEE, 2013, pp. 2053–2060.

[47] D. Whitley, S. Rana, J. Dzubera, and K. E. Mathias, "Evaluating evolutionary algorithms," *Artificial intelligence*, vol. 85, no. 1-2, pp. 245–276, 1996.

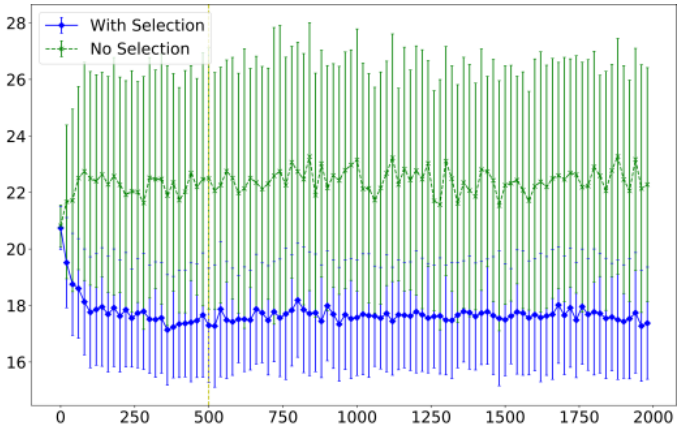

Fig. 15: Starting from the fitness and modularity optimal GRNs, the GRNs generated evolution demonstrated much fewer edges than the previous two-stage GRNs.

[48] M. L. Siegal and A. Bergman, "Waddington's canalization revisited: developmental stability and evolution," *Proceedings of the National Academy of Sciences*, vol. 99, no. 16, pp. 10 528–10 532, 2002.
[49] J. Masel, "Genetic assimilation can occur in the absence of selection for the assimilating phenotype, suggesting a role for the canalization heuristic," *Journal of evolutionary biology*, vol. 17, no. 5, pp. 1106–1110, 2004.
[50] S. Ciliberti, O. C. Martin, and A. Wagner, "Robustness can evolve gradually in complex regulatory gene networks with varying topology," *PLoS computational biology*, vol. 3, no. 2, p. e15, 2007.
[51] S. Huang, "Gene expression profiling, genetic networks, and cellular states: an integrating concept for tumorigenesis and drug discovery," *Journal of molecular medicine*, vol. 77, no. 6, pp. 469–480, 1999.
[52] S. Bhide, N. John, and M. R. Kabuka, "A boolean neural network approach for the traveling salesman problem," *IEEE Transactions on Computers*, vol. 42, no. 10, pp. 1271–1278, 1993.
[53] K. Gurney, *An introduction to neural networks*. CRC press, 2014.
[54] J. H. Holland *et al.*, *Adaptation in natural and artificial systems: an introductory analysis with applications to biology, control, and artificial intelligence*. MIT press, 1992.
[55] R. D. Leclerc, "Survival of the sparsest: robust gene networks are parsimonious," *Molecular systems biology*, vol. 4, no. 1, p. 213, 2008.
[56] M. E. Newman and M. Girvan, "Finding and evaluating community structure in networks," *Physical review E*, vol. 69, no. 2, p. 026113, 2004.
[57] N. Kashtan and U. Alon, "Spontaneous evolution of modularity and network motifs," *Proceedings of the National Academy of Sciences*, vol. 102, no. 39, pp. 13 773–13 778, 2005.
[58] Z. Qin, T. Gedeon, and R. I. McKay, "Why don't the modules dominate?" in *Proceedings of the Genetic and Evolutionary Computation Conference Companion*. ACM, 2018, pp. 121–122.